TÉCNICO LISBOA

Point of Care Platelet Counter

Joana Maria Andrade Tudela Martins

Thesis to obtain the Master of Science Degree in

Biomedical Engineering

Supervisors: Prof. Cláudia Alexandra Martins Lobato da Silva
Dr. André do Rosário Magalhães

Examination Committee

Chairperson: Prof. Maria Margarida Campos da Silveira
Supervisor: Prof. Cláudia Alexandra Martins Lobato da Silva
Member of the Committee: Dr. Ana Luísa Pecurto Cartaxo

October 2021

I declare that this document is an original work of my own authorship and that it fulfills all the requirements of the Code of Conduct and Good Practices of the Universidade de Lisboa. The work presented in this thesis was performed at the company Biosurfit, SA (Azambuja, Portugal), during the period March-December 2020, under the supervision of André Magalhães. The thesis was co-supervised at Instituto Superior Técnico by Prof. Cláudia Lobato da Silva.

Acknowledgments

Quero agradecer à Biosurfit, ao André Magalhães, Pedro Gomes, Maria João Costa que me acompanharam durante este processo, pela oportunidade e pela ajuda que estavam sempre prontos a dar. Foi uma experiência em tempos difíceis, mas sempre me fizeram sentir acompanhada.

Quero muito agradecer aos meus pais e avó, por me terem suportado e aturado quando estava stressada e nervosa por o projecto não correr bem, e por nunca terem parado de acreditar que eu iria conseguir.

Abstract

To answer the demand for faster turnaround times between sample collection and results in medical testing, haematological point of care devices have been rising in popularity. In this work, a proof of concept for an automated visual method of detecting platelets in images as a basis for a point of care device is presented. This work presents the design and development of the optical system needed to acquire the images, the sample treatment necessary to prepare the glass slides, the template-matching-based algorithm for object detection, and a preliminary analysis of the correlation, precision and bias of the two methods.

The first method, Manual counting, has the technician manually count each acquired image for platelets, while the second method, Algorithm counting, makes use of the template-matching algorithm to perform the object detection step. Both these methods will be compared to reference values obtained through traditional blood analysis methods.

Both methods showed a very strong positive correlation with the reference, as well as acceptable imprecision and bias values. The developed optical system performed up to standard and the acquired images had high enough quality to be used in both assessments. This work has proven to be a positive first step towards the development of the first point of care platelet counter.

Keywords

Point-of-Care; Platelet; Object Detection; Template-Matching; Optical Systems;

Resumo

De forma a responder à procura de maior rapidez entre a acquisição de uma amostra e os resultados da análise, aparelhos hematológicos 'point-of-care' têm subido em popularidade. Este trabalho pretende demonstrar um conceito para um contador de plaquetas 'point-of-care' automático, baseado na detecção de plaquetas em imagens. Este trabalho apresenta o sistema óptico desenhado para a aquisição de imagens, o tratamento das amostras necessário para preparar as lâminas que serão analisadas, um algoritmo de detecção de objectos baseade em 'template-matching', e uma análise preliminar da correlação, precisão e bias de dois métodos utilizados para a contagem de plaquetas.

O primeiro método, Manual counting, consiste no técnico contar manualmente o numero de plaquetas em cada imagem adquirida, enquanto que o segundo método, Algorithm counting, utiliza o algoritmo de deteção de objectos para realizar a contagem de plaquetas nas imagens. Para ambos os métodos, os resultados obtidos são comparados com os valores de referência das amostras utilizadas. Ambos os métodos demonstraram uma forte correlação positiva com a referência, assim como valores aceitáveis de imprecisão e bias. O sistema óptico desenvolvido funcinou como esperado e as imagens adquiridas tinham qualidade elevada o suficiente para serem utilizadas em ambos os métodos. Este trabalho demonstrou ser um primeiro passo positivo em direção ao desenvolvimento do primeiro dispositivo 'point-of-care' para a contagem de plaquetas.

Palavras Chave

'Point-of-Care'; Plaquetas; Detecção de Objectos; 'Template-Matching'; Sistemas Ópticos;

Contents

1 Introduction **1**

1.1 Motivation . . . 3

1.2 Objectives . . . 4

1.3 Thesis Outline . . . 4

2 Platelets: an Overview **5**

2.1 Platelets . . . 7

2.2 Image-based Platelet Counting . . . 7

3 The Optical Simulation **9**

3.1 Paraxial Setup and Ray Tracing . . . 11

3.2 MTF and Spot Diagram . . . 13

4 Experimental Setup **15**

4.1 Optical Microscope . . . 17

4.2 Sample Preparation . . . 19

4.3 Object Detection Algorithm . . . 20

5 Results and Discussion **21**

5.1 Image Quality . . . 23

5.1.1 Focus vs. Off Focus Images . . . 23

5.1.2 Microscope Performance . . . 24

5.2 Manual Platelet Counting . . . 26

5.3 Automated Platelet Counting . . . 28

5.3.1 Validation of proof of concept . . . 29

6 Conclusion **33**

6.1 Conclusion . . . 35

6.2 Future Work . . . 35

List of Figures

2.1 Platelet contributions to thrombus formation. Taken from [1] 7

3.1 Schematic representation of the planned optical setup. The LED is one of 3 possible LED. 11
3.2 Output of the paraxial analysis. 12
3.3 Lens Ray Tracing obtained with OSLO EDU. 12
3.4 Estimated MTF for the developped optical system. 13
3.5 Spot Diagram analysis for the developped optical system. 14

4.1 Microscope built for the project. 17
4.2 Comparision between all 3 LED light sources, when plane of focus is the plane where the platelets are located 18
4.3 Comparision between all 3 LED light sources, when plane of focus is not the plane where the platelets are located 18
4.4 Acquired image of red blood cells using the violet LED. the darker coloring is due to the fact that haemoglobin reacts to light in the violet emission range. 19

5.1 An Off Focus and Focus Image captured in the same FOV 23
5.2 Image acquired without a glass slide, to illustrate the problems with the camera, as well as the plastic disk.. 25
5.3 How the location of the microbead affects image quality, and highlight of the optical aberrations present in the optical system. 26
5.4 Calibration curve constructed from the values in table 5.2. 27
5.5 Image representation of the output of the objected detection algorithm through template matching. Objects surrounded by a green square have been positively identified as platelets by the algorithm. 28
5.6 Calibration curve constructed from the values in table 5.3. 29
5.7 Coefficient of Variation for all replicants used in both the manual and algorithm method. . 30
5.8 Statistical bias determined for each replicant. 30

List of Tables

5.1 Results obtained for images taken Off Focus and on Focus. 24
5.2 Average platelet count per field of view manually determined, compared to the reference value. 27
5.3 Results obtained for images after using an object detection through template matching algorithm. 28

Acronyms

CNN Convolutional Neural Network

CV Computer Vision

FOV Field of View

MTF Modular Transfer Function

PoC Point of Care

POTC Point of Care Testing

1

Introduction

Contents

1.1 Motivation 3

1.2 Objectives 4

1.3 Thesis Outline 4

In traditional laboratory testing, the sample is collected from a patient, then transported to a specialized laboratory for analysis, and then the results are reported back to the doctor. The turnaround time between sample collection and testing, as well as somewhat frequent errors that can occur in between the two processes, such as sample degradation, or misplacement, and wrong labelling, among others, can jeopardize the health, or in more extreme cases, the life of patients. [2].

The development of point–of–care testing (POCT) rose in popularity due to the ever-increasing demand for shorter turnaround times in test results. POCT is defined as rapid testing for diagnosis performed at or near the patient's bedside and can provide great value in areas with limited or non–existent access to laboratory devices. [3]. The shorter turnaround times, coupled with the diminishing or abolishment of the errors that can occur between sample collection and testing, allows for rapid decision-making regarding treatment, all with the hope of improving patient care.

Point of Care (POC) devices are usually small in size and low in weight, thus requiring low power consumption. They require a smaller amount of samples and reagents to deliver the same test results, making them more cost and patient-friendly. Furthermore, the short turnaround time implies that the results obtained through POCT more accurately reflect the state of the patient at the moment, and not a few hours or days before, making them especially useful in cases where patients need constant monitoring. Lastly, PoC devices are usually user-friendly require a short amount of training to be properly handled, which allows them to be handled by health care professionals, as well as the patients themselves in some cases. [3, 4]

POCT technology is advancing at a pace where the quality of the results delivered by a POCT device is on par with standard laboratory analysers. This level of quality propels the growing confidence in POCT devices and contributed to the increasing uptake of this equipment, especially in a secondary care setting. [2, 4]

1.1 Motivation

Most POCT devices related to haematology are related to haemoglobin concentration measurements, with some being used for red blood cell indices, as well as white blood cell count [3]. Haematology assays are of the utmost importance when it comes to evaluating one's health state, as they are one of the main resources used by medical professionals to detect health anomalies. However, the typical blood analysis procedure can be both time and labour consuming, and prone to the same errors as traditional laboratory testing, not to mention it requires the existence of such a facility, to begin with [5].

The fast output of POCT makes them extremely desirable in the haematology field, where clinical decisions need to be immediate or emergency scenarios where the patient requires constant monitoring. Moreover, the POCT's ability to provide low-cost reliable results, in the vicinity of the patient, and without

the need for specialists to be operated, is another great advantage. Currently, Biosurfit, SA has released the microfluidic PoC platform *spinit*® and three types of disposable discs are already available in the market: *spinit* CRP, *spinit* BC, and *spinit* HbA1c .

1.2 Objectives

In this work, a proof of concept for a POCT platelet counter is presented. The main objectives of this work are to develop a single-lens optical microscope with image quality on par to standard microscopes, where platelets can be easily distinguished and identified, to establish a standardized method of sample preparation that is representative of the whole blood sample, and to develop an image segmentation and object detection algorithm to identify and count platelets.

The goal of this work is to present the groundwork for a PLT count test for the *spinit*®.

1.3 Thesis Outline

This work is divided into six different chapters, in this section, a summary of each chapter is presented.

The first chapter, ”Introduction”, introduces the topic of POCT devices, their relevance in a secondary clinical setting, and the main objectives of this work.

The second chapter, ”Platelets: an overview”, presents a brief description of platelets, as well as a state of the art review of the methods used to identify platelets in a laboratory setting.

The third chapter, ”Optical Simulation”, presents the work done prior to the assembly of the microscope, explaining the parameters the optical set-up must possess.

In the fourth chapter, ”Experimental Setup”, an overview of the optical set-up assembled, sample preparation, and image processing method is presented. It is the main goal of this chapter to familiarize the reader with the microscope developed as well as the tests used to evaluate its performance.

The fifth chapter, ”Results and Discussion”, includes the performance of manual count of platelets and the object detection algorithm for independent samples and a complete analysis of the system developed. The main goal is to discuss the system performance, as well as improvements that need to be made to replicate this set-up in a *spinit*®.

The sixth and final chapter, ”Conclusion and future work”, presents a review of the developed device and suggestions for the next steps in the development.

2

Platelets: an Overview

Contents

2.1 Platelets 7
2.2 Image-based Platelet Counting 7

2.1 Platelets

Platelets, or thrombocytes, are small, non-nucleated blood cells, whose functions are essential to the normal process of hemostasis. They are small biconvex oval cells with diameters varying between 1.5 μm to 3.5 μm, with numbers in circulating blood varying between 150 and 450 Giga platelets per litre of whole blood [6]. In a blood spread, platelets tend to partially clump together, making their shape hard to distinguish, even with a proper staining technique.

As seen in figure 2.1, in the normal process of hemostasis, platelets will adhere to the collagenous tissue of the damage site, forming a plug that will later be reinforced with fibrin. In the second stage, platelets will promote blood clotting as they provide a surface for the adhesion and assembly of coagulation protein complexes. Lastly, platelets also express factors that are essential to modulate coagulation as well as vascular repair. [6]. Lack of circulating platelets, or thrombocytopenia, lead to a bleeding tendency, while the excess of platelets, or thrombocytosis, increases the risk of inappropriate blood clotting. Most inherited problems with platelet function are associated with either defect in the secretion of factors necessary for the hemostasis process, or defects in the expression of cell adhesion proteins [1].

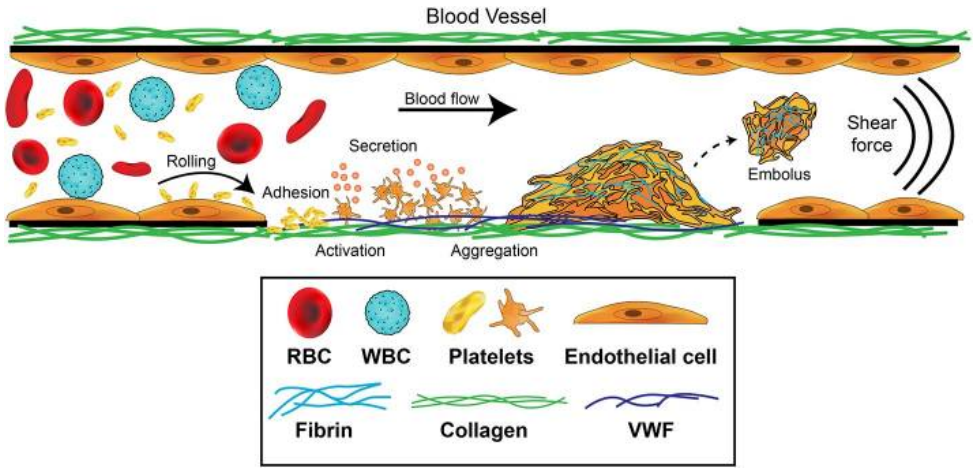

Figure 2.1: Platelet contributions to thrombus formation. Taken from [1]

2.2 Image-based Platelet Counting

Until the recent growth of haematology analysers, the reference method for platelet counting was the manual phase microscopy method, which was time-consuming, imprecise at low counts and often subjective method [7]. Even as automated haematology analysers grow in popularity and usage, manual counting of platelets is still widely used in laboratories that lack access to specialized instrumentation, or under-resourced laboratories. Furthermore, due to the imprecision of automated haematology

analysers for a situation of thrombocytopaenia, manual platelet counting is still widely used in clinical laboratories. [8].

Manual platelet counting has been replaced with automated haematology analyzers. There are commercial analyzers with several different methods of counting platelets, such as aperture impedance, optical scattering, fluorescence, and imaging [8]. All automated methods used for platelet counting must be precise, accurate over repeated samples, and give linear results over the entire analytical range. However, at higher counts, there's a probability of two or more cells passing through the sensing zone at the same time, and at lower counts, electric noise might be considered as a platelet. Lastly, the results obtained with similar method analysers on the same sample should be comparable.

Image-based platelet counting identifies individual blood cells based on morphology, and use a precise volume of blood to perform rapid image analysis. For example, the cobas M511 (Roche) [9] performs a complete blood count, whole blood counts, differential and reticulocyte counts using automatically printed and stained micro slides [8].

Most image-based systems use brightfield microscopy to identify the specimen. As the name suggests, brightfield microscopy is based on the fact that a bright viewing field will contrast with the specimen placed between the microscope's light source and objective lens. This type of microscope is simple to use, however, most specimen will require staining to be properly identified since brightfield microscopy doesn't alter the colour of the specimen [10]. Furthermore, brightfield microscopy can be coupled with digital imaging to obtain high-resolution images of the stained specimen. The main disadvantages of the brightfield technique are the inherently low contrast without staining, the need for a strong light source which may cause heat damage to the specimen, and the fact that the user needs to be knowledgeable in proper staining techniques.

In a blood smear with Giemsa staining, the platelets' cytoplasm is stained purple and has a granular appearance. This appearance is due to the concentration of organelles in the centre of the cell, which makes the edges of the cell poorly stained and very difficult to identify [1, 6]. Without staining, platelets appear as dark spots when they're in the field of focus, or as bright spots when the plane of focus is slightly above the plane where the platelets are located. Since it is always recommended to use a proper staining technique, little explanation of this phenomenon can be found in the literature. This phenomenon will be further explored in the following chapter when the optical setup used is explained.

3

The Optical Simulation

Contents

3.1 Paraxial Setup and Ray Tracing 11
3.2 MTF and Spot Diagram 13

The optical brightfield microscope developed for this project was based on the microscope currently present in the *spinit*® BC v.3 device. For the microscope to obtain a magnification of 20x, the eyepiece will consist of a singular achromatic aspheric lens, with a focal length, f, equal to 4.5 mm and a 3 mm diameter; the illumination source is planned to be either a green, violet, or red light emission diode (LED), and to focus the light in a singular beam, two condenser lenses were placed between the specimen and the LED. All images will be recorded using a Chameleon USB2 (ICX445 Mono). A schematic of the brightfield microscope is present in figure 3.1.

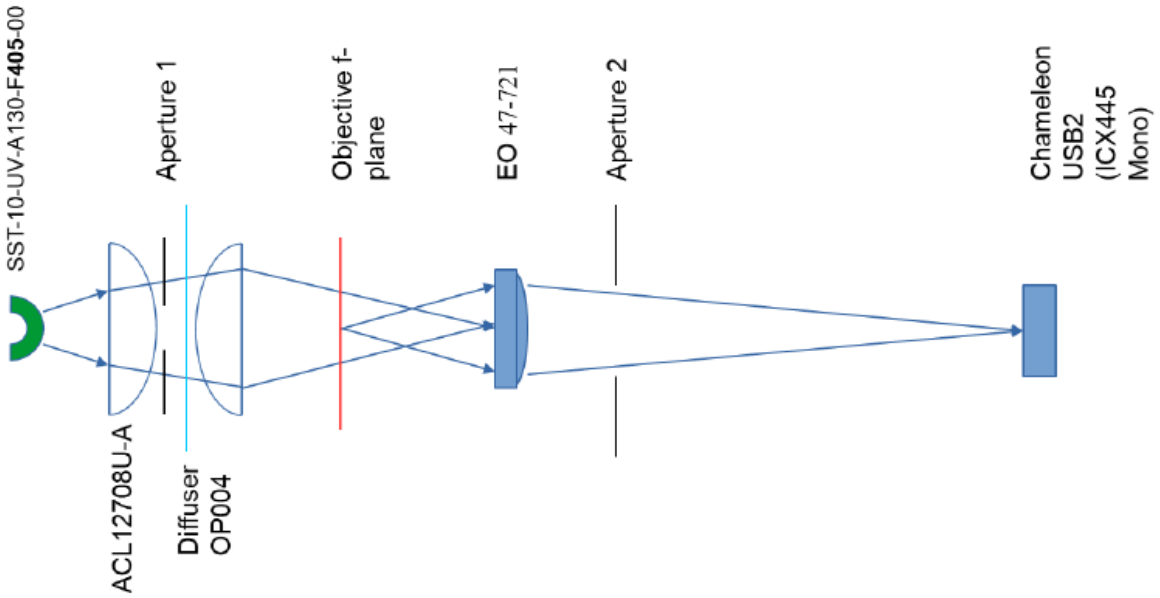

Figure 3.1: Schematic representation of the planned optical setup. The LED is one of 3 possible LED.

3.1 Paraxial Setup and Ray Tracing

The optical train of this microscope consists of an achromatic aspheric lens EO 47-721 and the eye is replaced by a Chameleon USB2 (ICX445 Mono). Before testing this lens in practice, a simulation of this lens performance was done using the student version of the software OSLO EDU. The desired magnification is 20x and knowing the lens specifications, it is possible to simulate the paraxial set-up of the lens.

The paraxial setup spreadsheet seen in figure 3.2 summarizes the aspects of the system that affect the paraxial properties of a lens. The OSLO EDU software divides these aspects into three categories: aperture, field, and conjugates. For this simulation, the known variables were the aperture sizes, the distance between the light source and the camera, the lens specifications, and desired magnification. With this information, we can solve for the object distance, which the software defines as the distance

*PARAXIAL SETUP OF LENS

APERTURE			
Entrance beam radius: *	0.700000	Image axial ray slope:	-0.148828
Object num. aperture:	0.007441	F-number:	3.215142
Image num. aperture:	0.148823	Working F-number:	3.359686
FIELD			
Field angle:	-1.461487	Object height: *	2.400000
Gaussian image height:	-0.120000	Chief ray ims height:	-0.119589
CONJUGATES			
Object distance:	94.068616	Srf 1 to prin. pt. 1:	0.456573
Gaussian image dist.:	3.082887	Srf 5 to prin. pt. 2:	-1.643372
Overall lens length:	3.200000	Total track length:	100.333583
Paraxial magnification:	-0.050000	Srf 5 to image srf:	3.064968
OTHER DATA			
Entrance pupil radius:	0.700000	Srf 1 to entrance pup.:	--
Exit pupil radius:	0.779019	Srf 5 to exit pupil:	-2.151485
Lagrange invariant:	0.017859	Petzval radius:	-6.320204
Effective focal length:	4.501199		
SPOT DIAGRAMS			
Aperture divisions:	17.030000	Gaussian apod. spec.:	Off
X 1/e^2 entr. irrad.:	1.000000	Y 1/e^2 entr. irrad.:	1.000000

Figure 3.2: Output of the paraxial analysis.

between surface 0, the camera, and surface 1, the lens, as well as the Gaussian image distance, which in our case is the distance between the lens and the specimen.

Now that the paraxial properties of the lens have been defines and studied, it's now possible to draw the ray interactions with the lens, as seen in Figure 3.3. Ray tracing is one of the best tools to evaluate optical lens performance before finalizing the design [11].

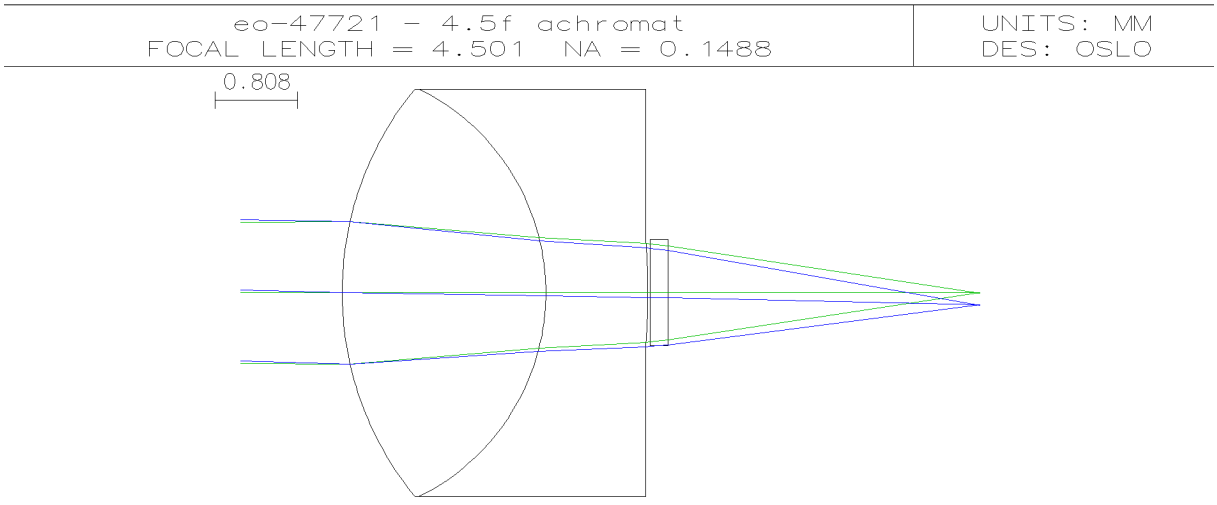

Figure 3.3: Lens Ray Tracing obtained with OSLO EDU.

3.2 MTF and Spot Diagram

After evaluating the lens ray tracing, should also look at the Modular Transfer Function (MTF) of the lens. In traditional system integration, the system's performance is estimated using the principle of the weakest link, which proposes that a system's resolution is solely limited by the component with the lowest resolution [10]. However, the quality of an image is determined by all the system's components, not just the component that yields the lowest resolution. In an optical system, the image quality is often characterized by transfer functions: the Fourier transform of the system's impulse response. Transfer functions are a powerful tool for analyzing optical systems since the transfer function of a complex optical system can be defined as the product of the transfer functions of each subcomponent. One of the most common transfer functions used to describe image quality is the MTF that is associated with every component of the system. The MTF is a performance-based specification of an optical system, described as the output to input ratio of modulation depth, for all spatial frequencies.

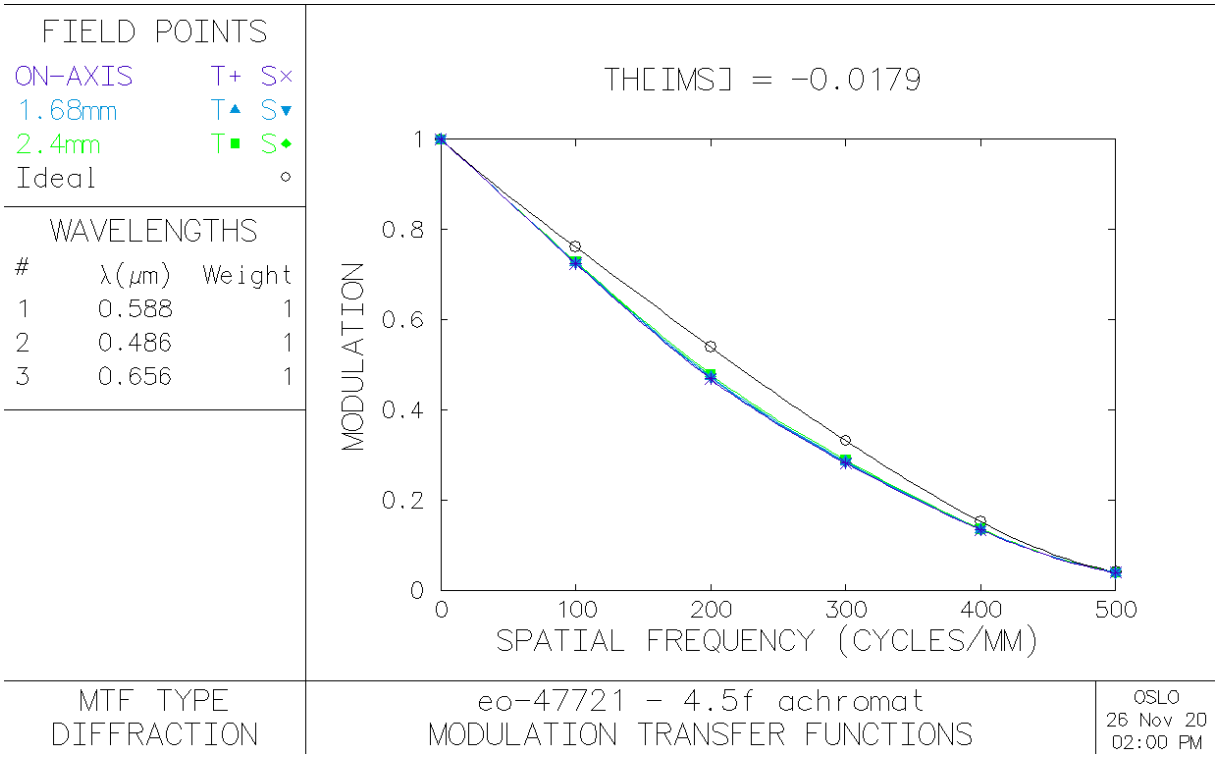

Figure 3.4: Estimated MTF for the developped optical system.

Spot diagrams are used to evaluate the presence of optical aberrations in an optical system [12]. Optical aberrations occur when light is spread over a region instead of focused on a single point. As seen in figure 3.5, there are no indications of the presence of an optical aberration in the system.

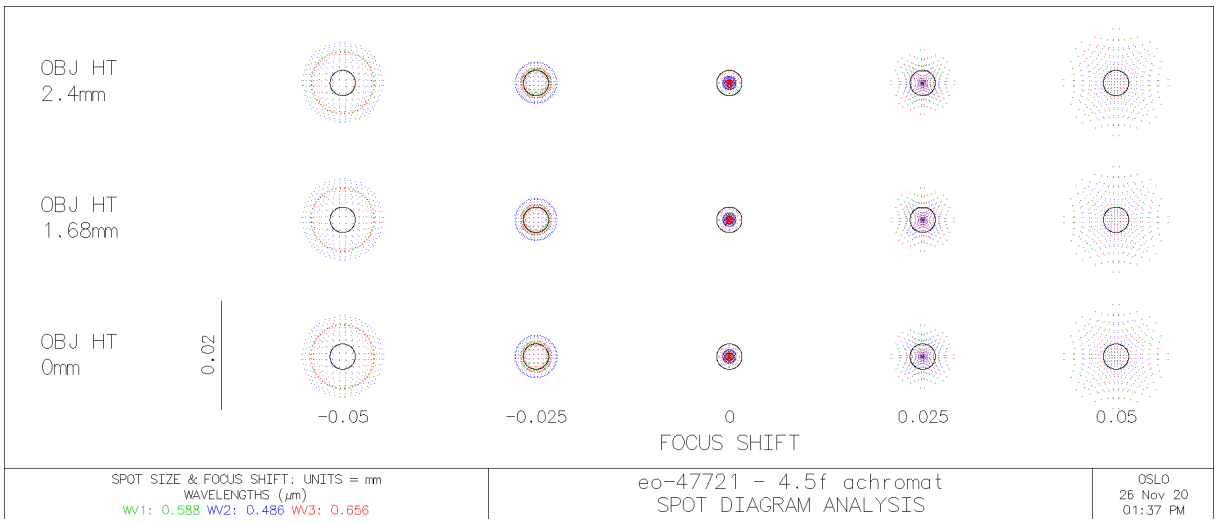

Figure 3.5: Spot Diagram analysis for the developped optical system.

With this analysis complete, the next step is to build the optical system that will be used throughout the entire report.

4

Experimental Setup

Contents

4.1 Optical Microscope 17

4.2 Sample Preparation 19

4.3 Object Detection Algorithm 20

The experimental set-up consists of the optical microscope built based on the specifications detailed in Chapter 3, the sample preparation performed before the sample was observed under the microscope and, lastly, the object detection algorithm based on template matching developed specifically for this proof of concept. In this chapter, each of the experimental set-up components will be presented and explained. Thus, this section is divided into 3 subsections.

4.1 Optical Microscope

Based on the simulations presented in Chapter 3, the built microscope is shown in figure 4.1.

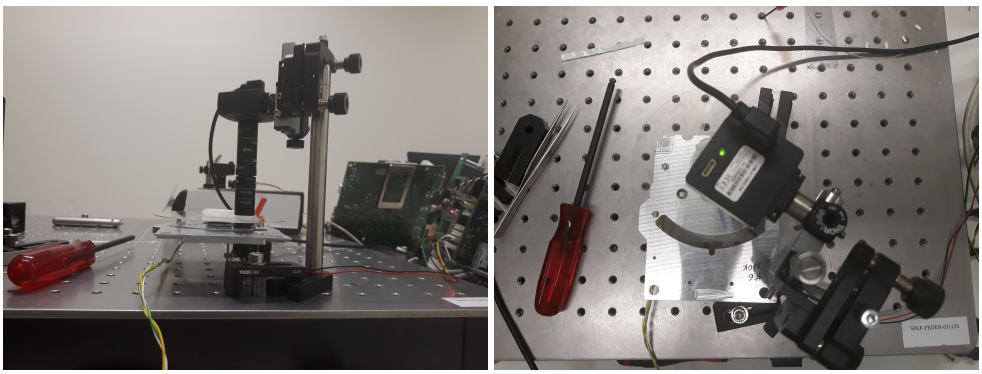

(a) (A) View from the front **(b)** (B) View from above

Figure 4.1: Microscope built for the project.

From the frontal view, the camera is located at the top, supported by a mechanical arm with one knob that controls the position of the camera in the z-axis (silver knob seen in the top view). The aspherical lens is located at the end of the tube, with the aperture located at the halfway point of the tube. After the end of the tube, there's a metal disk support, with a clear plastic disk placed on it and secured to the support so it can rotate, but not move along the z-axis. At the end of the circular gap, there's a small container which is where the LED is connected, as well as two more aspheric lenses that will serve as a light collimator. After the glass slide is prepared, it is placed on top of the disk. To alter the FOV, all that must be done is gently rotate the disk by hand.

For the colour of the LED, originally there were 3 options of colour for the LED light: red, green, or violet. In the figure below, the 3 differences in results between the 3 types of light sources are presented, for both focused, and non focused platelets.

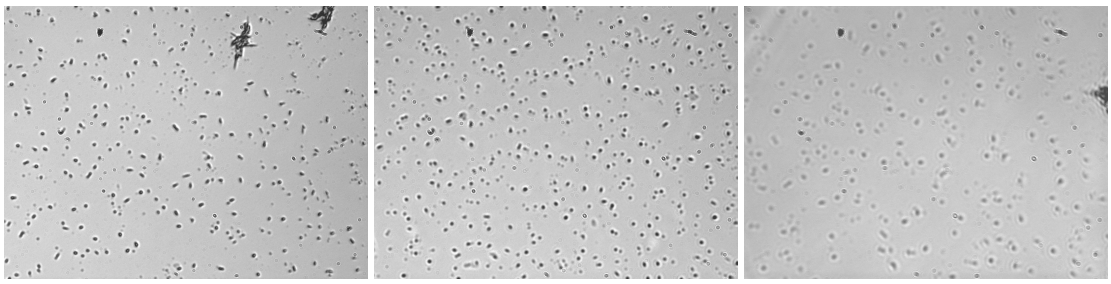

(a) Violet LED **(b)** Green LED **(c)** Red LED

Figure 4.2: Comparision between all 3 LED light sources, when plane of focus is the plane where the platelets are located

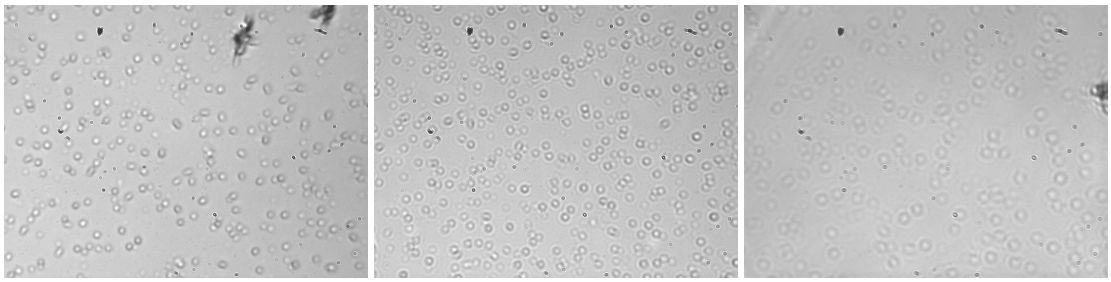

(a) Violet LED **(b)** Green LED **(c)** Red LED

Figure 4.3: Comparision between all 3 LED light sources, when plane of focus is not the plane where the platelets are located

From the figures 4.2 and 4.3, there's a clear improvement in image quality as the LED's emitting wavelength decreases. The shutter speed of the camera also increases as the wavelength of the LED increased, meaning the required time for an image acquisition increases. Furthermore, the curious light-emitting effect the platelets display when out of focus is more noticeable for shorter wavelengths as well. Although there's little information in the literature about this curious effect, it is believed to occur due to light that is diffracted and culminates in what is referred to as the out of focus plane, producing a lens effect. Furthermore, and keeping future improvements in mind, the violet LED interacts with the haemoglobin present in red blood cells, staining these types of cells a lot darker than usual, as can be seen in figure 4.4.

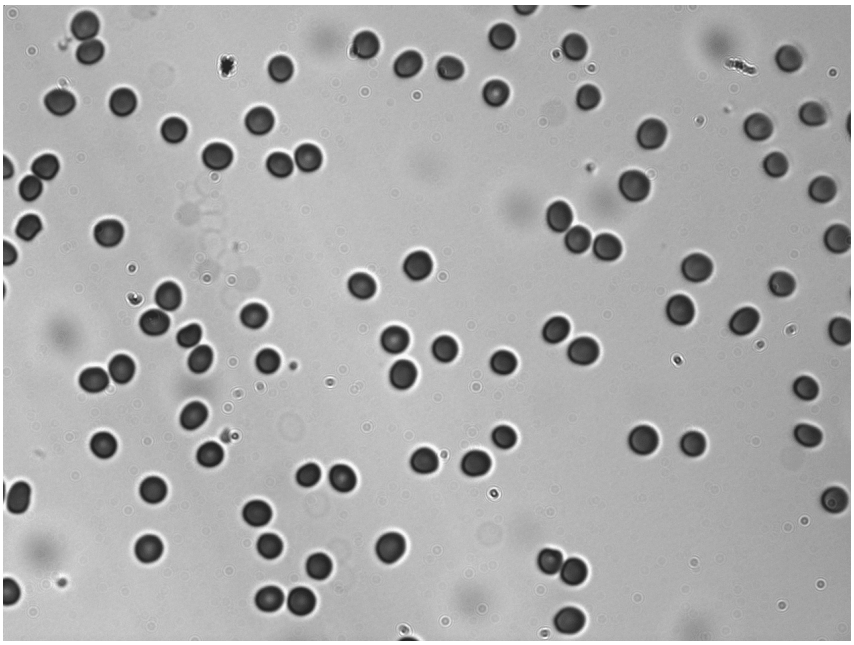

Figure 4.4: Acquired image of red blood cells using the violet LED. the darker coloring is due to the fact that haemoglobin reacts to light in the violet emission range.

4.2 Sample Preparation

For this proof of concept, venous blood samples used in this work had a complete blood count report associated with each of them. This report had been obtained using traditional blood analysis techniques. From the transport time, the blood inside the vials had partially sedimented, leaving 3 distinct layers: a plasma and platelets layer at the top, a red blood cell layer at the bottom, and a layer with mostly white blood cells in between the two. All sample preparation was done in a laminar flow cabinet.

1. From the middle of the first layer, retrieve 90μL of plasma from the blood vial and transfer it to an Eppendorf tube.
2. From a solution containing microbeads, NaCL 0.4% and blue staining dye, transfer 10μL of the microbead solution to the Eppendorf and gently stir the Eppendorf tube. The microbead solution is used as a tool to help focus the images later on.
3. Transfer 10μL of the Eppendorf's solution to a glass slide and gently cover it with a glass slip.

After preparing the glass slip, it was transferred to the microscope. Using the software *FlyCapture*, images were manually focused before capture. For each image, initially, two images with two different planes of focus were acquired. For each glass slide, images from 5 different regions were acquired. Each acquired image had to contain at least one microbead.

This process was repeated twice for each sample.

4.3 Object Detection Algorithm

Computer vision (CV) is the field that enables computers and systems to identify and classify meaningful information from images, videos, and other visual inputs, and acts accordingly to the information it received [13]. To do so, CV makes use of two essential techniques: deep learning machine learning algorithms and convolutional neural networks. Both these techniques require a lot of resources, as well as computing power to process huge sets of visual information, including a large image database for learning and testing the implemented technique. CV allows for several tasks related to digital analysis process. For this proof of concept, object detection is the CV task used to identify and classify platelets.

Object detection is defined as a CV technique whose purpose is to locate and identify objects within an image, or another type of visual input, by drawing bounding boxes are the specified objects. As is the case for all CV tasks, the techniques usually used to perform object detection are deep learning algorithms and CNN. However, it is possible to object detection without using such resource-heavy techniques: by using template matching.

The digital technique for finding small parts of an image that matches a given template image is known as template matching in digital image processing. This solution is more simple than using a deep learning algorithm or a CNN, with the additional advantage of not requiring data to be annotated, and of requiring less computational power for the same accuracy in simple objects. Thus, the algorithm chosen for this proof of concept is a simple template matching algorithm.

The template matching algorithm was implemented in python used the open-sourced computer vision library, *OpenCV*. The algorithm is based on the premise that a template is compared to a base image in every pixel in the image. The output of this comparison is a map of similarities, where the higher the score, the higher the likelihood of your template being in that pixel. For this work, 5 templates created from 5 platelets were used and each template was compared against the image twice: once at full size, and once at 95% of the size. To be considered a match, the similarity score had to be above the predefined threshold, 0.85.

5

Results and Discussion

Contents

5.1 Image Quality 23

5.2 Manual Platelet Counting 26

5.3 Automated Platelet Counting 28

In the fifth chapter, all the results obtained throughout the development of this early model are presented and analysed. This chapter will thus be divided into 3 subsections which are:

1. Image Quality, where the two types of focus were tested and one focus was chosen to be used throughout the rest of the project, as well as analyse the shortcomings of the optical system built and where it needs improvement.
2. Manual Platelet Counting, where it's performed the preliminary analysis to determine whether or not a relationship exists between the average number of platelets seen in an image and the referenced number of platelets of a sample.
3. Automated Platelet Counting, where the algorithm developed is tested and the obtained results are analysed to determine whether or not they follow the trend seen in the manual analysis, as well as compare the performance of both and discuss the reasons behind the different results.

5.1 Image Quality

5.1.1 Focus vs. Off Focus Images

After the introduction of the microbeads into the sample to be observed under the microscope, there were two possible planes of focus: one where the focal points are the platelets, which will be referred to as the focus plane, and one where the focal points are the microbeads, which will be referred to as Off Focus because the platelets are off focus. Figure 5.1 highlights the differences between the two preliminary focus methods used.

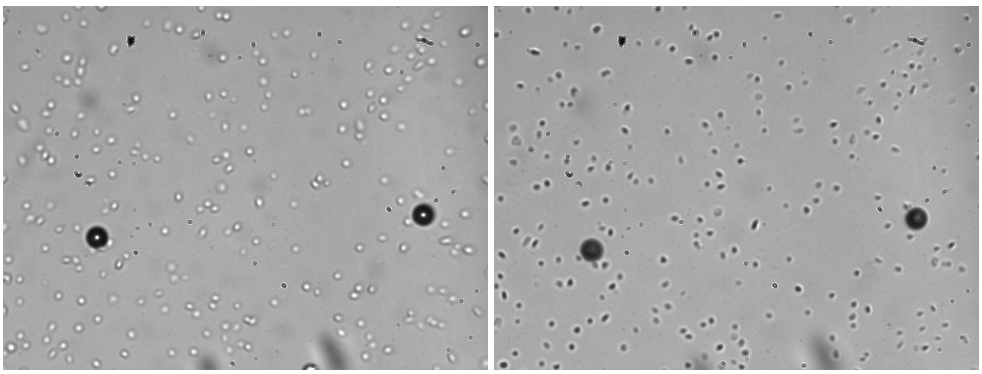

(a) Example of an Off Focus Image **(b)** Example of a Focus Image

Figure 5.1: An Off Focus and Focus Image captured in the same FOV

To manually count all the platelets seen in each FOV, the public licensed Java program ImageJ was used (documentation on ImageJ [14]). Among its many features, imageJ allows the user to mark

objects, in this case, platelets, numbering them as new marks are added. Thus, it is easier to count manually all the platelets using ImageJ, than it is by counting them by hand. For the case of Focus type images, all the objects that were small, dark, and of circular shape, were considered to be platelets. On the other hand, for the Off Focused type images, the objects that had a bright centre, a round shape, were small, as well as had a distinguishable border were classified as platelets. The results are present in the table below 5.1.

Table 5.1: Results obtained for images taken Off Focus and on Focus.

Sample	Average Off Focus	Average Focus
1	108.7	108.4
2	119.6	120.5
3	163.7	164.1
4	181	181.3
5	198	197.5
6	213	212.6
7	232.9	233.1
8	261.9	260.4
9	263.3	262.2

As we can see from table 5.1, there isn't a significant difference between the two methods. The main observable differences occur because platelets are in motion, even when placed in a glass slide, thus, the time it took to shift from one focal plane to another is enough to cause the slight differences. However, some of the differences also occurred due to the fact that small debris was mistakenly classified as platelets in focus-type images, due to their similarities in shape and size. Since platelets become light points, when the focal plane is the microbeads plane, debris were more easily distinguished from platelets in the Off Focus-type images. Furthermore, by using microbeads as the focal reference, it's possible to always use the same focal plane through all samples and measures. This isn't the same for images in the Focus category since platelets are a lot smaller than the height of the volume present in the glass slide.

With all this taken into consideration, the Off Focus type images were the ones used throughout the rest of the analysis, in order to minimize as many as possible errors of human nature.

5.1.2 Microscope Performance

In regards to the image quality, some issues must be underlined. First of all, the camera lens has some debris in it that cannot be removed, so, the camera would've had to be replaced to fix this issue. Furthermore, the plastic disk itself also accumulated some degree of debris, which couldn't be completely

cleaned with the methods at hand. Of course, these aren't issues that would remain in the *spinnit* version of the platelet counter, due to the natural differences between the two concepts. However, this did affect the results and the analysis, introducing a new layer of errors that could not be changed or fixed.

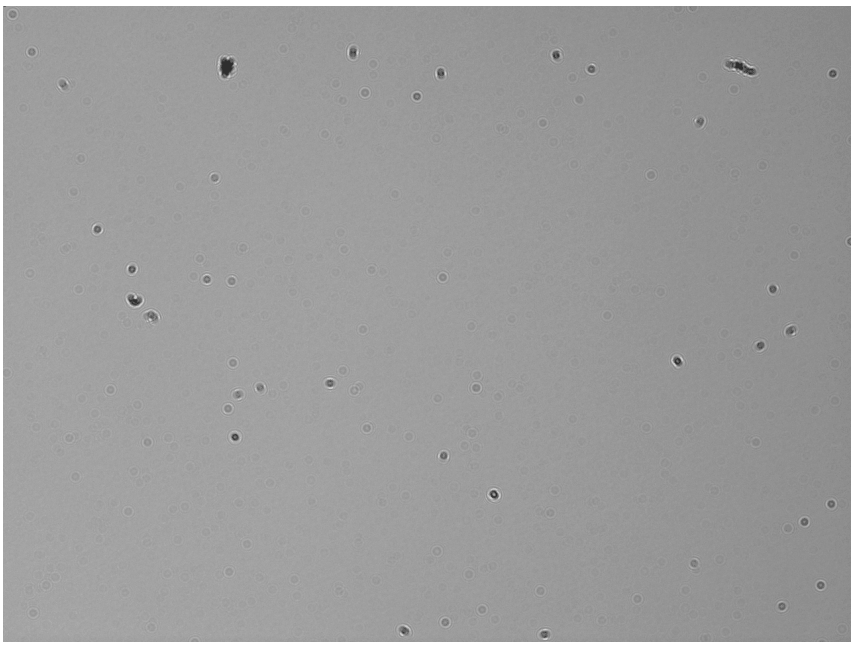

Figure 5.2: Image acquired without a glass slide, to illustrate the problems with the camera, as well as the plastic disk..

Moving on to the aspheric lens itself, it improved the spherical aberration present in previous iterations of this microscope. However, it's possible to see some degree of spherical aberration as well as astigmatism in this optical set-up as well. These optical aberrations are more prominent when the microbead used to focus is located near the edges of the field of view.

All the highlighted issues will influence the manual and algorithm results, although wherein manual analysis there is human supervision to distinguish these issues, the algorithm may struggle to correctly detect platelets in this scenario.

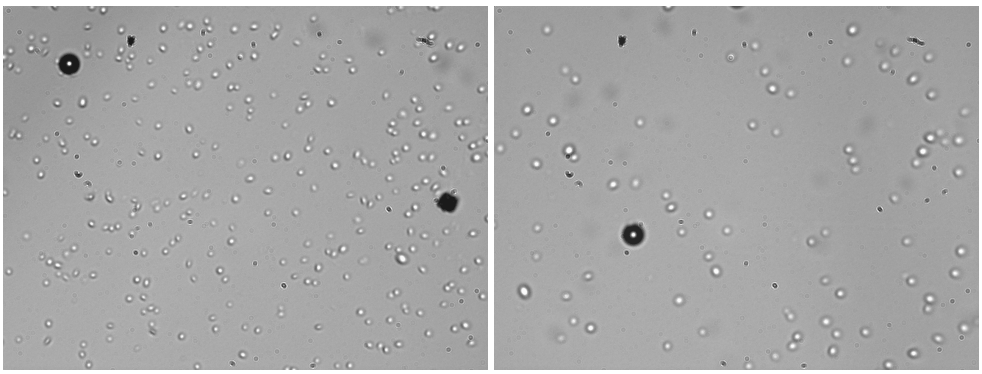

(a) Bead is located in the top left corner, which results in objects losing their circular shape

(b) Bead is located in the center, which results in objects keeping their circular shape

Figure 5.3: How the location of the microbead affects image quality, and highlight of the optical aberrations present in the optical system.

5.2 Manual Platelet Counting

Once it was established that the type of images to be used was the Off Focus images, it was time to evaluate whether or not the 5 FOV could be used to estimate the number of platelets present in a traditional blood analysis. In order to do so, 9 samples with reference values ranging from 152 to 397 were used; none of the samples used to belong to people whose blood tests revealed abnormal flags or complications. Each sample was used twice, and the average of all counts was used to infer a correlation between the average number of platelets per field of view and the reference value.

Before counting, the visual criteria to what objects were classified as platelets was established:

- Platelets are small and circular objects, characterized by a bright centre surrounded by a border that was darker than the background of the image.
- Due to the presence of debris in the camera lens that could not be cleaned, if an object that met point 1 was totally or partially obscured by darker debris, then it would not be classified as a platelet.
- Additionally, due to the presence of debris in the glass slides, if an object that met point 1 was located in a shaded area, where the brightness of its centre could no longer be distinguished, then it would not be classified as a platelet.

With these criteria clearly defined, each FOV for each sample was counted and recorded in a table for further analysis. A summary of the average number of platelets seen per FOV for each sample is present in Table 5.2.

Table 5.2: Average platelet count per field of view manually determined, compared to the reference value.

Sample	Reference (x10^9PLT/L)	Average (PLT/FOV)
1	152	108.7
2	182	119.6
3	246	163.7
4	268	181
5	280	198
6	306	213
7	338	232.9
8	360	261.9
9	397	263.3

The values present in Table 5.2 have a Pearson's correlation value, R, equal to 0.9915, which implies that there's a near-perfect positive correlation between the average number of platelets seen per FOV and the platelet reference value of the original sample. Once this correlation has been established, the reference value a sample has can be estimated from the average number of platelets seen in 5 distinct FOV. Using linear regression, the calibration curve present in figure 5.4 was created.

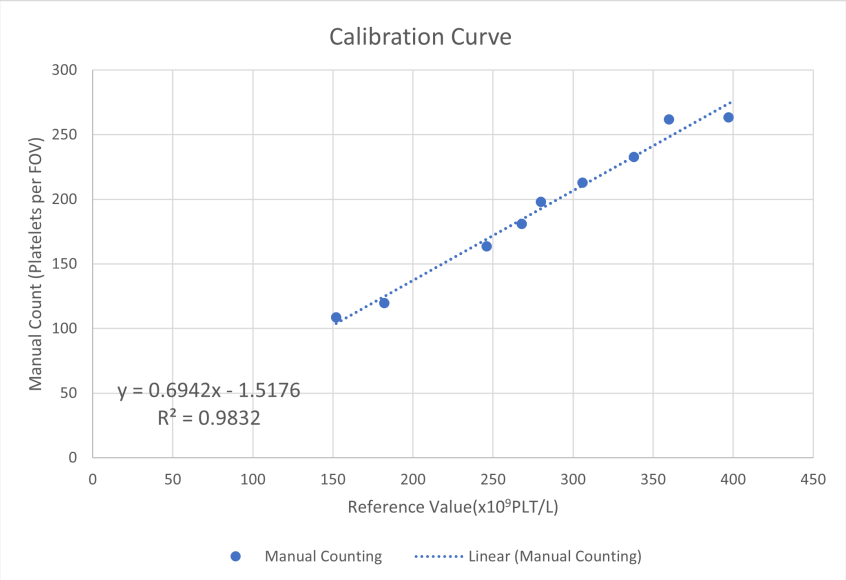

Figure 5.4: Calibration curve constructed from the values in table 5.2.

With the equation of the calibration curve, it's then possible to extract the standard deviation, coefficient of variation, as well as bias.

5.3 Automated Platelet Counting

For this subsection, each captured image used for manual counting ran through the object detection algorithm implemented for this project, and the final count values were extracted to a spreadsheet to be analysed through the same tools like the ones obtained through manual counting. First of all, a representation of the output of the algorithm is present in Figure 5.5.

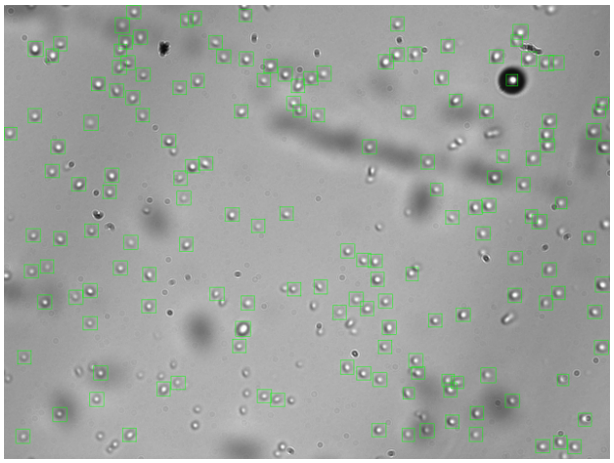

Figure 5.5: Image representation of the output of the objected detection algorithm through template matching. Objects surrounded by a green square have been positively identified as platelets by the algorithm.

As we can see from figure 5.5, almost all objects identified as platelets through manual counting have been identified as platelets by the algorithm. However, the more noticeable exceptions were the microbead added to help find the right focus plane was also classified as a platelet by the algorithm; objects that were too close together, or overlapped partially, were not classified as platelets, and objects present in shaded areas were classified as platelets by the algorithm. A summary of the obtained outputs are present in Table 5.3.

Table 5.3: Results obtained for images after using an object detection through template matching algorithm.

Sample	Reference (x10^9PLT/L)	Average Algorithm
1	152	104.7
2	182	123.3
3	246	142.6
4	268	191.9
5	280	213.8
6	306	197
7	338	225.6
8	360	254.3
9	397	241.9

The values present in Table 5.3 have a Pearson's correlation value, R, equal to 0.9528, which implies that there's a strong positive correlation between the average number of platelets seen per FOV and the platelet reference value of the original sample. As was the case for manual counting, once this correlation has been established, the reference value a sample has can be estimated from the average number of platelets detected by the algorithm in 5 distinct FOV. Using linear regression, the calibration curve present in figure 5.4 was created.

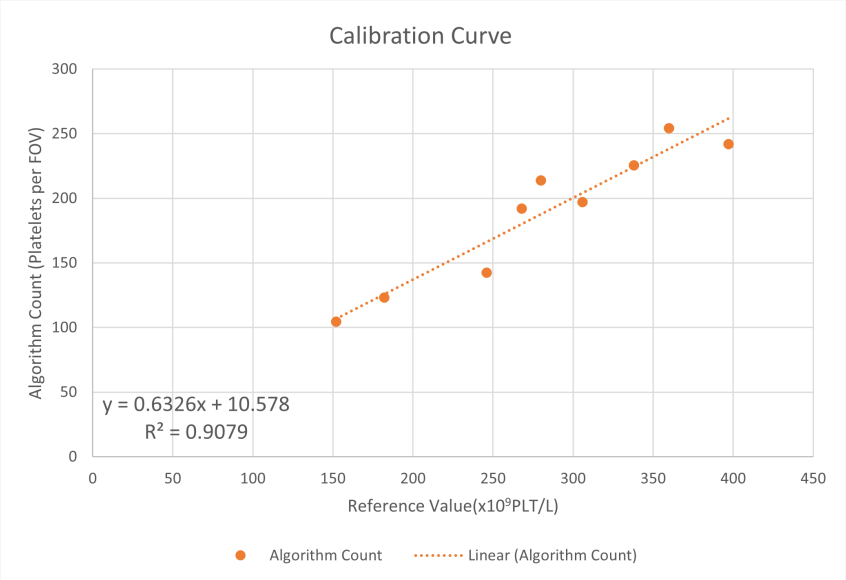

Figure 5.6: Calibration curve constructed from the values in table 5.3.

Unlike in Figure 5.4, there's a higher deviation from the estimated calibration curve and the output from the algorithm.

5.3.1 Validation of proof of concept

In this subsection, the aim is to discuss the precision and validity of the method comparison used for this proof of concept. First and foremost, although 2 replicants were used per sample and the samples covered a clinically meaningful range, the number of samples used was too low. the Australasian Association of Clinical Biochemistry [15] recommends the use of at least 40 samples between both methods and, even including the replicants, this proof of concept out contained 9 samples.

When it comes to evaluating the precision of the method, all replicants were used in this analysis. Starting with the standard deviation, the manual method presents a lower average standard deviation ($SD = 14.65$) than the algorithm method ($SD = 25.22$). In percentual terms, the coefficient of variation follows the same trend: the manual method shows a $CV(\%) = 8.19\%$, while the algorithm analysis shows a $CV(\%) = 13.68\%$. For a preliminary method, these values are promising and show the reproducibility

of the methods in this proof of concept.

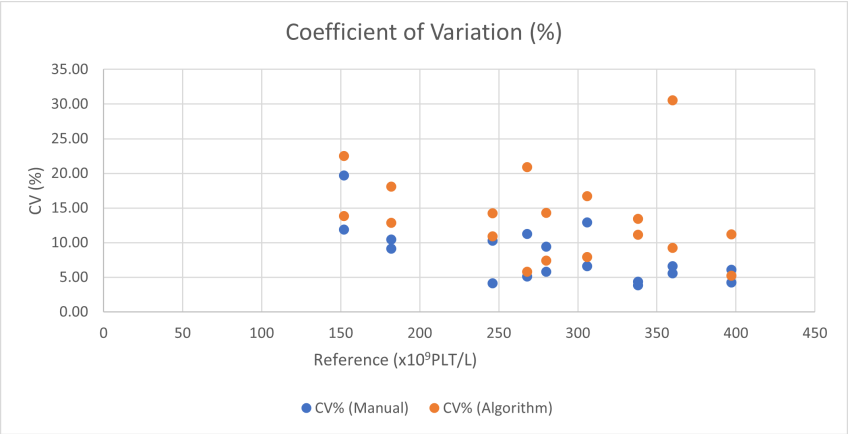

Figure 5.7: Coefficient of Variation for all replicants used in both the manual and algorithm method.

As expected, the manual method shows an overall lower standard deviation and coefficient of variation than the algorithm method. This occurs mostly due to the fact that there is no human supervision in the algorithm method, while in the manual method it is possible to discern platelets when the microbead is located too close to the edge of the FOV. Overall these results are acceptable but could be improved in future iterations of this method.

As for the statistical bias of the methods presented, both methods do not display a clear bias, as seen by figure 5.8, with the overall bias being 0.39 for the manual object detection method and -2.80 for the algorithm-based object detection. Both values are within the acceptable range.

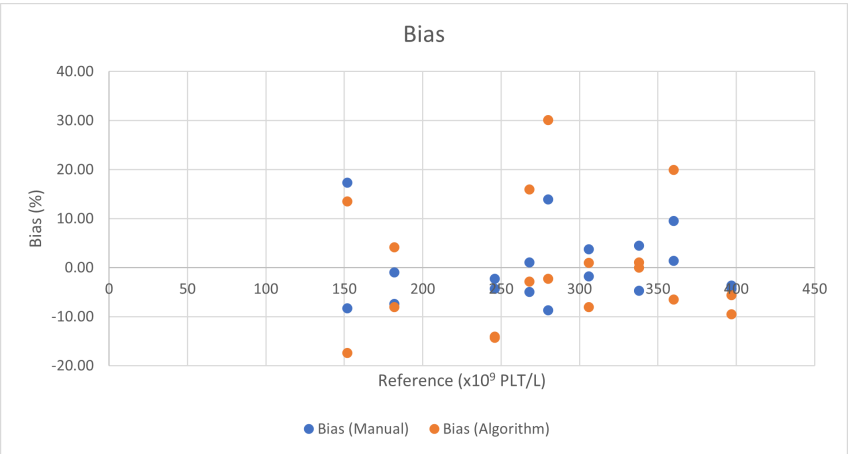

Figure 5.8: Statistical bias determined for each replicant.

Lastly, this discrepancy between the manual method and algorithm method is also due to the fact that there was no outlier treatment performed. As mentioned previously, the algorithm couldn't properly identify platelets in scenarios where the microbead was too close to the edge of the FOV. If these in-

stances were to be removed from the analysis, then it is highly likely that the correlation values, standard deviation, as well as coefficient of variation would improve and, perhaps, make this difference between the two methods tinier.

6

Conclusion

Contents

6.1 Conclusion 35

6.2 Future Work 35

6.1 Conclusion

In traditional laboratory testing, the sample is collected from a patient, then transported to a specialized laboratory for analysis, and then the results are reported back to the doctor, which may take too long and jeopardize the well-being of patients. The rise of POCT in popularity as an answer to this demand for shorter turnaround times brings new and inventive methods of testing that are accurate, fast, and can be done by the patient's bedside.

The aim of this work was to show a proof of concept for an automated PoC Platelet counter. This would be the first device of its type in the market and with the rise of PoC white blood cell counter, or in some cases, PoC complete blood counters, there's a window in the market for a medical device such as this.

The optical system is small, cheap, and easily recreated in other environments. The optical aberrations noticed in the image analysis didn't change the fact that both through manual object detection and template matching object detection there was a positive correlation between the number of platelets detected and the original sample value. This work was also demonstrated to be precise and unbiased in its results, as well as easily reproducible. Furthermore, it fits the criteria of a PoC device: it is small and only requires a small sample to perform its work, making it both cost and patient-friendly.

6.2 Future Work

As mentioned before, the main limitation of this work is the number of samples used to test the two methods. Although it was possible to infer some conclusions regarding the correlation, precision and bias of the method, a minimum of 40 samples would've been required if it were to prove this device was able to enter the market.

Furthermore, the sample acquisition method and treatment is still done outside of the device, the sample is still being treated by human hands when the image acquisition process occurs. The next few steps would be to either make the image acquisition process autonomous. Another future improvement is the transition from glass slides to a microchamber through where the blood would flow and platelets would be detected while in flow, instead of in static. This step would imply a redesign of the acquisition method, a newly design disk with microchambers specifically designed to allow the flow of platelets while removing other blood components.

As long as POCT continues to rise in popularity, it is the responsibility of the developers to ensure these tests deliver the same results as traditional methods, as well as help fill a need in society. Although this particular device still has a long journey ahead of itself, these are positive first steps towards a brighter future.

Bibliography

[1] S. J. Montague, Y. J. Lim, W. M. Lee, and E. E. Gardiner, "Imaging platelet processes and function-current and emerging approaches for imaging in vitro and in vivo," *Frontiers in immunology*, vol. 11, pp. 78–78, Jan 2020, 32082328[pmid]. [Online]. Available: https://pubmed.ncbi.nlm.nih.gov/32082328

[2] G. P. Zaloga, "Evaluation of bedside testing options for the critical care unit," *CHEST*, vol. 97, no. 5, pp. 185S–190S, May 1990. [Online]. Available: https://doi.org/10.1378/chest.97.5_Supplement.185S

[3] C. Briggs, S. Kimber, and L. Green, "Where are we at with point- of- care testing in haematology?" *British Journal of Haematology*, vol. 158, no. 6, pp. 679–690, 2012. [Online]. Available: https://onlinelibrary.wiley.com/doi/abs/10.1111/j.1365-2141.2012.09207.x

[4] C. Briggs, D. Guthrie, K. Hyde, I. Mackie, N. Parker, M. Popek, N. Porter, and C. Stephens, "Guidelines for point-of-care testing: haematology," *British Journal of Haematology*, vol. 142, no. 6, pp. 904–915, 2008. [Online]. Available: https://onlinelibrary.wiley.com/doi/abs/10.1111/j.1365-2141.2008.07274.x

[5] J.-N. Kuo and B.-S. Li, "Lab-on-cd microfluidic platform for rapid separation and mixing of plasma from whole blood," *Biomedical Microdevices*, vol. 16, no. 4, pp. 549–558, Aug 2014. [Online]. Available: https://doi.org/10.1007/s10544-014-9857-1

[6] B. P. Young, *Wheater's functional histology : a text and colour atlas*. Fourth edition / by Barbara Young, John W. Heath ; with contributions by Alan Stevens, James S. Lowe ; drawings by Philip J. Deakin. Edinburgh ; New York : Churchill Livingstone, 2000., 2000, includes index.;System requirements for accompanying computer disc: Windows 95 or 98. [Online]. Available: https://search.library.wisc.edu/catalog/999908847202121

[7] H. C. Segal, C. Briggs, S. Kunka, A. Casbard, P. Harrison, S. J. Machin, and M. F. Murphy, "Accuracy of platelet counting haematology analysers in severe thrombocytopenia and potential

impact on platelet transfusion," *British Journal of Haematology*, vol. 128, no. 4, pp. 520–525, 2005. [Online]. Available: https://onlinelibrary.wiley.com/doi/abs/10.1111/j.1365-2141.2004.05352.x

[8] S. Kemble, C. Briggs, and P. Harrison, *Platelet Counting*, 4th ed. Academic Press (Elsevier), Mar. 2019, pp. 582–591.

[9] M. Bruegel, T. George, B. Feng, T. Allen, D. Bracco, D. Zahniser, and H. Russcher, "Multicenter evaluation of the cobas m 511 integrated hematology analyzer," *International Journal of Laboratory Hematology*, vol. 40, 07 2018.

[10] M. Bass, C. DeCusatis, J. Enoch, V. Lakshminarayanan, G. Li, C. Macdonald, V. Mahajan, and E. Van Stryland, *Handbook of Optics, Third Edition Volume I: Geometrical and Physical Optics, Polarized Light, Components and Instruments(Set)*, 3rd ed. USA: McGraw-Hill, Inc., 2009.

[11] W. J. Smith, *Chapter 3. Paraxial Optics and Calculations.*, 4th ed. McGraw-Hill Education, 2007, p. 35–51.

[12] "Interpreting lens spot diagrams," accessed: 2021-03-03. [Online]. Available: https://www.opticsforhire.com/blog/interpreting-spot-diagrams

[13] "IBM about computer vision," https://www.ibm.com/topics/computer-vision, accessed: 2020-12-03.

[14] "ImageJ documentation," https://imagej.nih.gov/ij/docs/index.html, accessed: 2020-12-08.

[15] "australasian association for clinical biochemistry and laboratory medicine." [Online]. Available: https://www.aacb.asn.au/